

# Effect of adding magnesium to lithium on the performance of discharge and hydrogen evolution of the lithium anode

Kanghua Chen · Ziyang Zhang · Erfu Ni

Received: 2 March 2009 / Accepted: 16 August 2009 / Published online: 1 September 2009  
© Springer Science+Business Media B.V. 2009

**Abstract** The present study evaluates the effect of magnesium as an inhibitor on the performance of discharge and hydrogen evolution of lithium anode in alkaline electrolyte with additives. The electrochemical behaviors of lithium and lithium–magnesium alloy are assessed by hydrogen evolution rate, discharge current density, anodic potential, and potentiodynamic polarization. For these conditions, the results show that addition of magnesium to lithium enhances the current efficiency. Addition of 0.07 wt% Mg to lithium has minor effect on discharge current and anodic potential of lithium anode. The chemical composition and the morphology of the anode surfaces were evaluated by X-ray diffraction and scanning electron microscopy. The results show that the slow dissolution of lithium–magnesium alloy generates the formation of LiOH, LiOH·H<sub>2</sub>O, and Mg(OH)<sub>2</sub>. After discharge in saturated alkaline electrolyte with additives, the lithium–magnesium surface is less porous than lithium surface. Hydrogen evolution decrease, prompted by adding magnesium to lithium, is related to surface integrity enhanced by Mg(OH)<sub>2</sub>.

**Keywords** Lithium–water battery · Lithium anode · Hydrogen evolution · Lithium–magnesium alloy · Passive film

## 1 Introduction

Lithium has the advantages of low density (0.534 g cm<sup>-3</sup>), more negative standard electrochemical potential (−3.05

V<sub>SHE</sub>) than any other metal elements, and high unit mass electrochemical equivalence (3.86 Ah g<sup>-1</sup>). A lithium battery has high specific energy and high specific power when lithium is used as the anode. The theoretical specific energy of the lithium is 11,148 Wh kg<sup>-1</sup> based on the Li/O<sub>2</sub> reaction, or 8,450 Wh kg<sup>-1</sup> based on the Li/H<sub>2</sub>O reaction. Consequently, it has profound applicable perspective in military and civil field when lithium is used as an electrode material. In lithium–water system, lithium is used as negative electrode and the positive electrode is a kind of material with less hydrogen overpotential such as nickel or stainless steel. When they are submerged in aqueous solution and connected with wire outside, the current occurs through the wire. This can be observed using amperometer. However, a direct chemical reaction between lithium and water occurs when lithium discharges: 2Li + 2H<sub>2</sub>O = 2LiOH + H<sub>2</sub>. Lithium suffers losses in the electrochemical reaction. As a result, the practical energy density and current efficiency of lithium decrease. Concurrently, hydrogen and heat are produced due to the reaction of lithium with water. The battery could explode severely [1]. Study on the electrochemical behaviors of lithium in alkaline aqueous solutions, and how to decrease the hydrogen evolution rate has been carried out by several research groups [1–21]. A porous lithium hydroxide film forms on lithium in contact with aqueous solutions [2–9]. The behavior of the hydrogen evolution reaction and the discharge performance are dependent on the property and integrity of the surface film when lithium discharges. The property and integrity of the surface film are affected by many factors, such as electrolyte temperature, concentration, and flow velocity. The lower the hydroxyl concentration, the higher the temperature and electrolyte flow velocity, the higher is the dissolution rate and the higher is the hydrogen evolution rate. The inhibitive efficiency of organic corrosion inhibitor decreases with

K. Chen · Z. Zhang (✉) · E. Ni  
State key Laboratory of Powder Metallurgy, Central South University, Lushan Road South, 410083 Changsha, China  
e-mail: zyzhang2003@yahoo.com

increasing temperature [10, 11]. A polymer membrane and ionic liquid have been used on the lithium anode surface. The parasitic corrosion reaction is inhibited with the very low discharge current density [14–16]. Alloying the lithium anode is the feasible means to modify the film property, to further reduce hydrogen evolution, and to optimize discharge performance of the lithium anode. However, study on alloying the lithium anode in aqueous alkaline solution has been scarce. Alloying the lithium anode with aluminum has been investigated. It is reported that the hydrogen evolution rate was reduced at the lithium–aluminum anode surface [20, 21]. However, the anodic efficiency suffered losses concomitant to inordinately low current density, only 200–300 mA cm<sup>-2</sup>. It is considered that the standard electrode potential of magnesium is near that of lithium, they have similar physical and chemical properties, magnesium atoms could dissolve in lithium in the form of solute atoms [22, 23], the solubility of magnesium hydroxide formed from magnesium in contact with alkaline aqueous solution is comparatively lower, and stabler than that of lithium hydroxide. In this project, the impact of adding a minor amount of magnesium to the lithium anode on the hydrogen evolution reaction, discharge performance, and surface film is studied.

## 2 Experimentation

### 2.1 Materials

Lithium metal bars (99.95%, 15 mm thick and 100 mm long, China JianZhong Nuclear Fuel Co. Ltd.) and magnesium metal ingot (99.96%) were used to prepare the lithium–magnesium alloys. Two lithium–magnesium alloys (Li–0.07 wt% Mg and Li–1.16 wt% Mg) were prepared in a resistance furnace using a stainless steel crucible in a dry argon atmosphere. The smelting temperature was controlled within 800–1,000 °C. Two phases (Li and Li<sub>3</sub>Mg<sub>7</sub>) were detected in the Lithium–magnesium alloys via XRD after the heat treatment (Fig. 1). The aqueous electrolyte was prepared from lithium hydroxide monohydrate (LiOH·H<sub>2</sub>O; AR 90%), sodium hydroxide (NaOH; AR 99.5%), and de-ionized water. The volume of the cell electrolyte was 2,000 mL of solution for each test. The solution was prepared to yield concentrations of 4 M (mol L<sup>-1</sup>), LiOH at 3.524 M, and NaOH at 0.476 M, respectively. In literature [11], the author used organic additives to reduce the parasitic direct corrosion reaction between lithium metal and the electrolyte. In order to obtain the better effect of hydrogen inhibition, we selected four additives as hydrogen inhibitors according to literature [11]: 0.3 M ethanol (AR 99.7%), 0.034 M triethanolamine (AR 90%), 0.03 M triethylene glycol (AR 90%), and 4.23 × 10<sup>-4</sup> M lead nitrate (Pb(NO<sub>3</sub>)<sub>2</sub> AR 90%) [24]. The former three additives reduce the activity

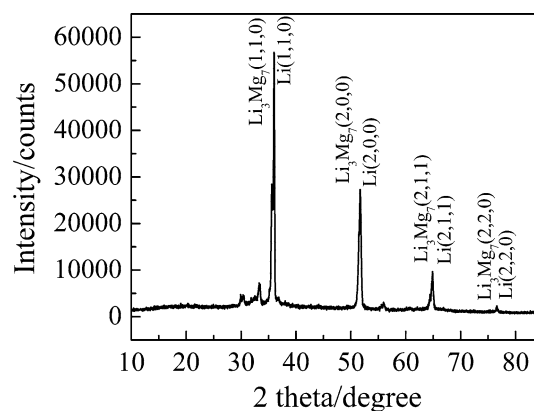


**Fig. 1** X-ray diffraction patterns of the lithium–magnesium alloy

of the water by forming inter-molecular hydrogen bonding between the organic additive and water. In the latter additive Pb enhanced hydrogen evolution overpotential of lithium anode.

### 2.2 Experimental setup

The experiments of discharge current and hydrogen evolution rate were performed utilizing the setup shown in Fig. 2. The lithium and lithium–magnesium alloy ingot were precast into foil 1.6 cm in diameter and 2 mm thick. The electrode foil was assembled in a cylindrical holder (exposed area 1 cm<sup>2</sup>). After acetones cleansing, the electrode was placed in the electrochemical setup. A stainless steel plate was used as the cathode which was placed at another end of the setup. The electrolyte was circulated through the pump and the fresh electrolyte was introduced from the bulk to the electrode surface. An inverted funnel

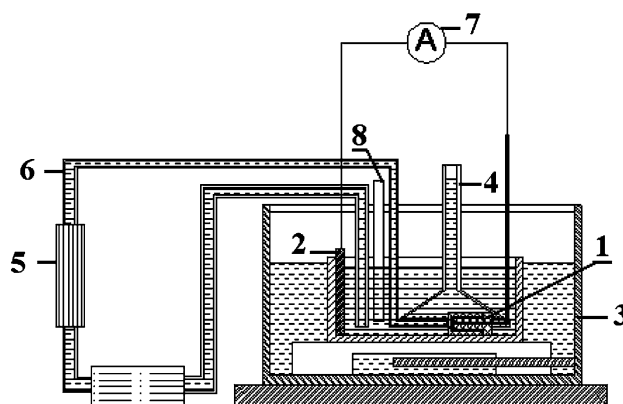


**Fig. 2** Schematic electrochemical setup used for electrochemical measurement of the anode. 1 Lithium anode, 2 stainless steel blade, 3 constant temperature water tank, 4 burette, 5 flowmeter, 6 electrolyte circulation system, 7 amperometer, and 8 thermometer

burette was placed above the anode in order to collect the evolved hydrogen. The current in the circuit was recorded by an amperometer. The whole electro-bath was placed in a constant temperature water bath box.

The anodic potential curves and polarization curves were determined in a classical three-electrode cell (Fig. 3). In this figure,  $V_1$ , and  $V_2$  are voltmeters used for measuring the potential between the anode and the counter electrode or the anode and the reference electrode, respectively. A stands for the amperometer used for measuring the current in the circuit, and  $R$  is the resistance in the circuit. The counter electrode was stainless steel plate. The standard calomel electrode (SCE) was contained within a separate compartment, in which there was saturated KCl solution. The standard calomel electrode was connected to the test cell via a salt bridge. The end of the salt bridge was made into a luggin probe, and the tip of the luggin probe was placed near the sample holder, at a distance of 0.4 cm from the anode surface. In potentiodynamic polarization experiment, the reference electrode is Hg/HgO electrode, which was directly submerged in the alkaline electrolyte. In Fig. 3, the electrochemical reactions at each electrode are as follows:

Lithium anode:  $\text{Li} \rightarrow \text{Li}^+ + e$

Stainless steel Cathode:  $\text{H}_2\text{O} + e \rightarrow \frac{1}{2}\text{H}_2 + \text{OH}^-$

The battery reaction:  $\text{Li} + \text{H}_2\text{O} \rightarrow \text{Li}^+ + \text{OH}^- + \frac{1}{2}\text{H}_2$

The parasitic corrosion reaction between lithium

and water:  $\text{Li} + \text{H}_2\text{O} \rightarrow \text{LiOH} + \frac{1}{2}\text{H}_2$

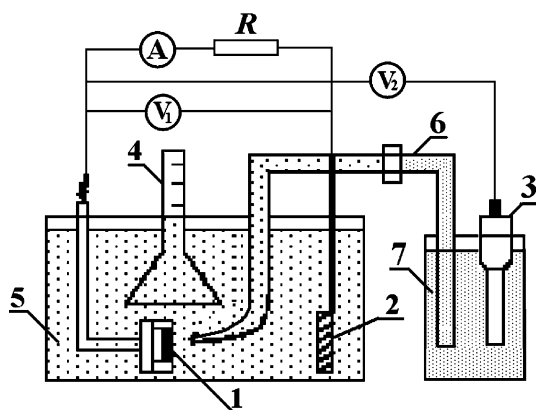


**Fig. 3** Schematic electrochemical setup used for electrochemical polarization of the anode. 1 Lithium anode, 2 stainless steel blade, 3 standard calomel electrode (SCE), 4 burette, 5 electrolyte, 6 salt bridge, 7 saturated KCl solution, 8 A—amperometer, 9  $V_1$ ,  $V_2$ —voltmeter, and 10  $R$ —resistance

### 3 Results

#### 3.1 The impact of adding magnesium to the lithium anode on the hydrogen evolution rate and discharge current of the lithium anode

The corrosion reaction of lithium in alkaline electrolyte is the bottleneck of lithium/water battery development. The corrosion reaction could be described by the hydrogen evolution rate at the lithium/solution interface. The anodic dissolution rate could be described by the discharge current density. The current efficiency of lithium/water battery is governed by the ratio of the above two competing reactions [3]. The hydrogen evolution rates of lithium with different content of magnesium in 4 M alkaline electrolyte at 30 °C are shown in Fig. 4. The decrease in rate with addition of magnesium to lithium is clearly evidenced. The hydrogen evolution rate at the Li–0.07 wt% Mg electrode was clearly lower than that at the lithium anode and the hydrogen evolution rate at the Li–0.07 wt% Mg electrode increases more slowly.

The hydrogen evolution rate at the Li–1.16 wt% Mg electrode was lower than that at the lithium anode at short notice, but the hydrogen evolution rate at the Li–1.16 wt% Mg electrode increased quickly with time increasing and near that at the lithium anode.

The discharge current densities of lithium with different content of magnesium in 4 M alkaline electrolyte at 30 °C are shown in Fig. 5. Evidently, the discharge current density at the lithium anode is stable at about  $530 \text{ mA cm}^{-2}$  in 5 min. Adding magnesium to the lithium anode does not markedly affect the discharge current density of the lithium anode. The discharge current density of the Li–0.07 wt% Mg alloy anode remained at about  $510 \text{ mA cm}^{-2}$  in 5 min

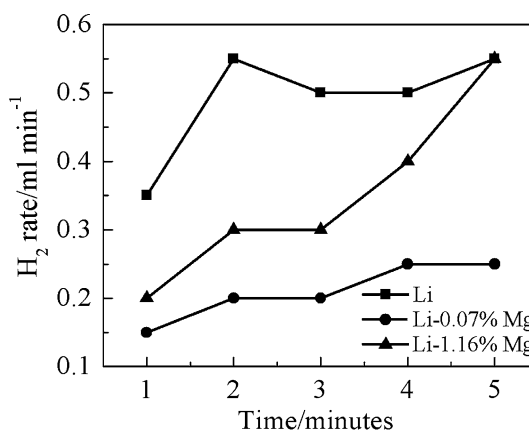


**Fig. 4** The hydrogen evolution rate of lithium and the lithium–magnesium alloy versus time at 30 °C. The points are experimental data. The anode used is indicated in the figure. The solution flow velocity was controlled at  $18 \text{ L h}^{-1}$

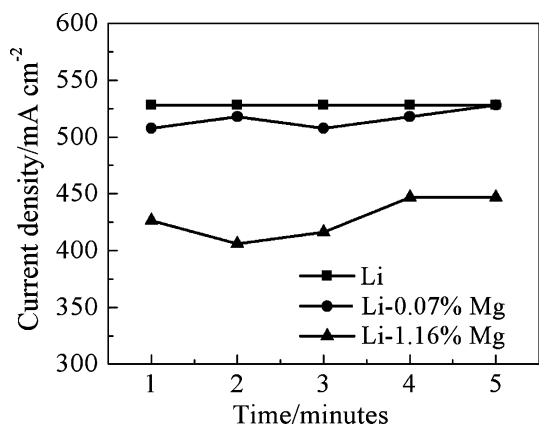


**Fig. 5** The current density of lithium and the lithium–magnesium alloy versus time at 30 °C. The points are experimental data. The anode used is indicated in the figure. The solution flow velocity was controlled at 18 L h<sup>-1</sup>

and eventually it nearly equaled 530 mA cm<sup>-2</sup>. The discharge current density of the Li–1.16 wt% Mg alloy anode remained between 425 and 450 mA cm<sup>-2</sup> in 5 min. Compared with the lithium anode, adding 1.16 wt% Mg to the lithium anode decreased the current density of anode more or less.

The current efficiencies of lithium with different content of magnesium in 4 M alkaline electrolyte at 30 °C are shown in Fig. 6. Clearly, the current efficiency of the Li–0.07 wt% Mg alloy is higher than that of lithium, which is approximately 92–96%. The efficiency of the Li–1.16 wt% Mg alloy is higher than that of lithium at the early stage and is near that of lithium as time increases due to the hydrogen evolution rate increase.

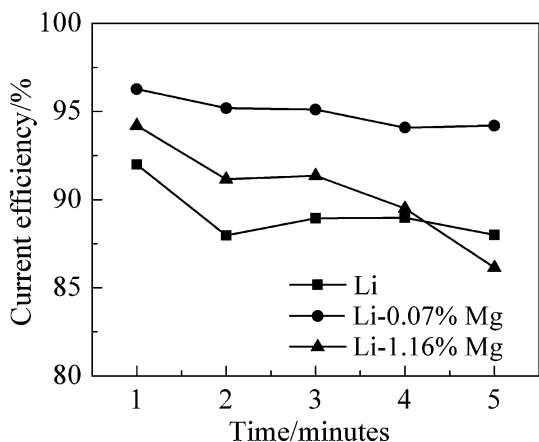


**Fig. 6** The current efficiency of lithium and the lithium–magnesium alloy versus time at 30 °C. The points are calculated data from that in Figs. 4 and 5. The anode used is indicated in the figure. The solution flow velocity was controlled at 18 L h<sup>-1</sup>

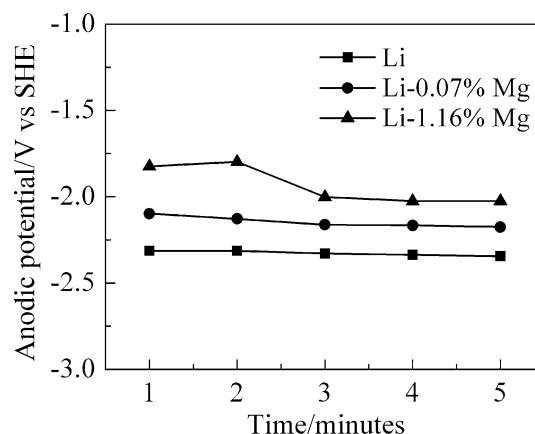


**Fig. 7** The anodic potential of lithium and the lithium–magnesium alloy versus time at 30 °C. The points are experimental data. The anode used is indicated in the figure. The solution flow velocity was controlled at 18 L h<sup>-1</sup>

### 3.2 The impact of adding magnesium to lithium anode on the anodic potential of lithium

The anodic potentials of lithium with different content of magnesium in 4 M alkaline electrolyte at 30 °C are shown in Fig. 7. The curves indicate that the anodic potential of the lithium anode shifts in the positive direction with addition of magnesium. The anodic potential of the lithium is stable at -2.3 V (vs. SHE). The anodic potential of the Li–0.07 wt% Mg is stable at -2.1 V (vs. SHE). There is a minor fluctuation during the period of discharge. The anodic potential of the Li–1.16 wt% Mg alloy is about -2.0 V (vs. SHE) and there is a slight fluctuation. It is stable after 3 min discharge.

### 3.3 The impact of adding magnesium to the lithium anode on the polarization of the lithium anode

In the presence of additives, the polarization curves of lithium and the lithium–magnesium alloy in the alkaline aqueous electrolyte are shown in Fig. 8. The open circuit potential ( $E_{ocp}$ ) and micro-cell corrosion current density ( $J$ ) derived from the curves are shown in Table 1. It can be seen that the anodic current density decreases, the cathodic current density increases, and the open circuit potential shifts in the positive direction with addition of magnesium. It shows that the anodic process is inhibited and the cathodic process is promoted with addition of magnesium.

Both the anodic polarization current density and the cathodic polarization current density have small changes with addition of 0.07 wt% Mg. The open circuit potential of Li–0.07 wt% Mg is a little more positive than that of lithium, which indicates that addition of 0.07 wt% Mg have a weak effect on the polarization of the lithium anode and cathode. Both the anodic polarization current density

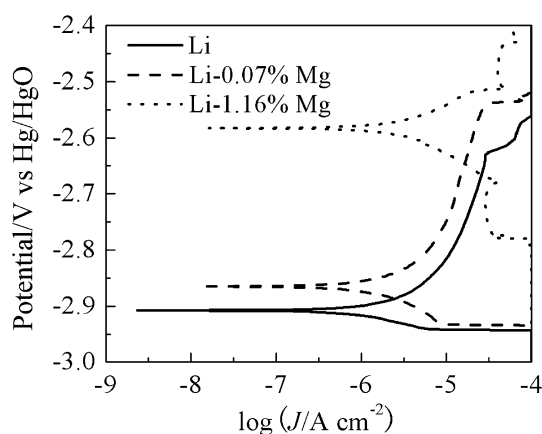


**Fig. 8** Effect of adding magnesium to lithium on polarization of the lithium anode. The temperature of the electrolyte is 30 °C; the flow-rate of the electrolyte is 18 L h<sup>-1</sup>. The reference electrode is Hg/HgO electrode

**Table 1** Corrosion parameters of lithium and lithium–magnesium alloy negative

Sample	$E_{\text{corr}}$ (V)	$J$ ( $\mu\text{A cm}^{-2}$ )
Li	-2.908	1.987
Li-0.07 wt% Mg	-2.865	2.594
Li-1.16 wt% Mg	-2.583	19.66

and the cathodic polarization current density show large changes with addition of 1.16 wt% Mg. The open circuit potential of Li-1.16 wt% Mg is higher than that of lithium. Addition of 1.16 wt% Mg to lithium reduced the activity of lithium. It is consistent with the large current discharge results of the lithium and lithium–magnesium alloy in Fig. 5.

Table 1 exhibits that the micro-cell corrosion current density of Li-0.07 wt% Mg is 2.594  $\mu\text{A cm}^{-2}$ , which is near the micro-cell corrosion current density of lithium (1.987  $\mu\text{A cm}^{-2}$ ). While the micro-cell corrosion current density of Li-1.16 wt% Mg is 19.66  $\mu\text{A cm}^{-2}$ , higher than that of lithium. It shows that addition of 1.16 wt% Mg to the lithium anode is apt to create micro-cell corrosion reaction, which leads to the higher micro-cell corrosion current of Li-1.16 wt% Mg.

### 3.4 The impact of adding magnesium to the lithium anode surface film

The anode surface film is the key factor which affects the discharge and hydrogen evolution behavior of the lithium anode. The preparation process of the anode surface film was as follows. The electrolyte used was saturated lithium hydroxide (5.3 M) in the trials due to the problematic lithium corrosion in dilute lithium hydroxide [4]. Sodium

hydroxide was added to the lithium hydroxide electrolyte to maintain the saturation of electrolyte. The additives used were the same as those stated above. Lithium and lithium–magnesium anode discharged in the setup (shown in Fig. 2) for a period of time. The anode was disassembled and quickly placed in a plastic bag filled with argon when gray film was created on the surface. The anode surface was immediately carried out analysis via X-ray diffraction (XRD) and scanning electron microscope (SEM).

#### 3.4.1 SEM results of analysis

In the presence of additives, SEM images of lithium in the saturated lithium hydroxide electrolyte and the Li-1.16 wt% Mg alloy in the saturated lithium hydroxide electrolyte containing sodium hydroxide after 12 h discharge are presented in Fig. 9a, b. It is noted from the SEM images that the surface film is porous. The surface film of lithium (Fig. 9a) is rough, loose, and porous. However, the surface film of Li-1.16 wt% Mg alloy (Fig. 9b) is comparatively compact and smooth. Magnesium was detected on the surface of the Li-1.16 wt% Mg alloy rather than on that of the lithium after discharge from the energy-dispersive X-ray spectrum (EDX; Figs. 9c, d). The distribution diagram of Mg on the surface of Li-1.16 wt% Mg is shown in Fig. 9e. It can be seen that the substance containing Mg on the surface is well-distributed. The substance created from Mg on the lithium–magnesium alloy surface after discharge distributes uniformly on the porous film.

#### 3.4.2 XRD results of analysis

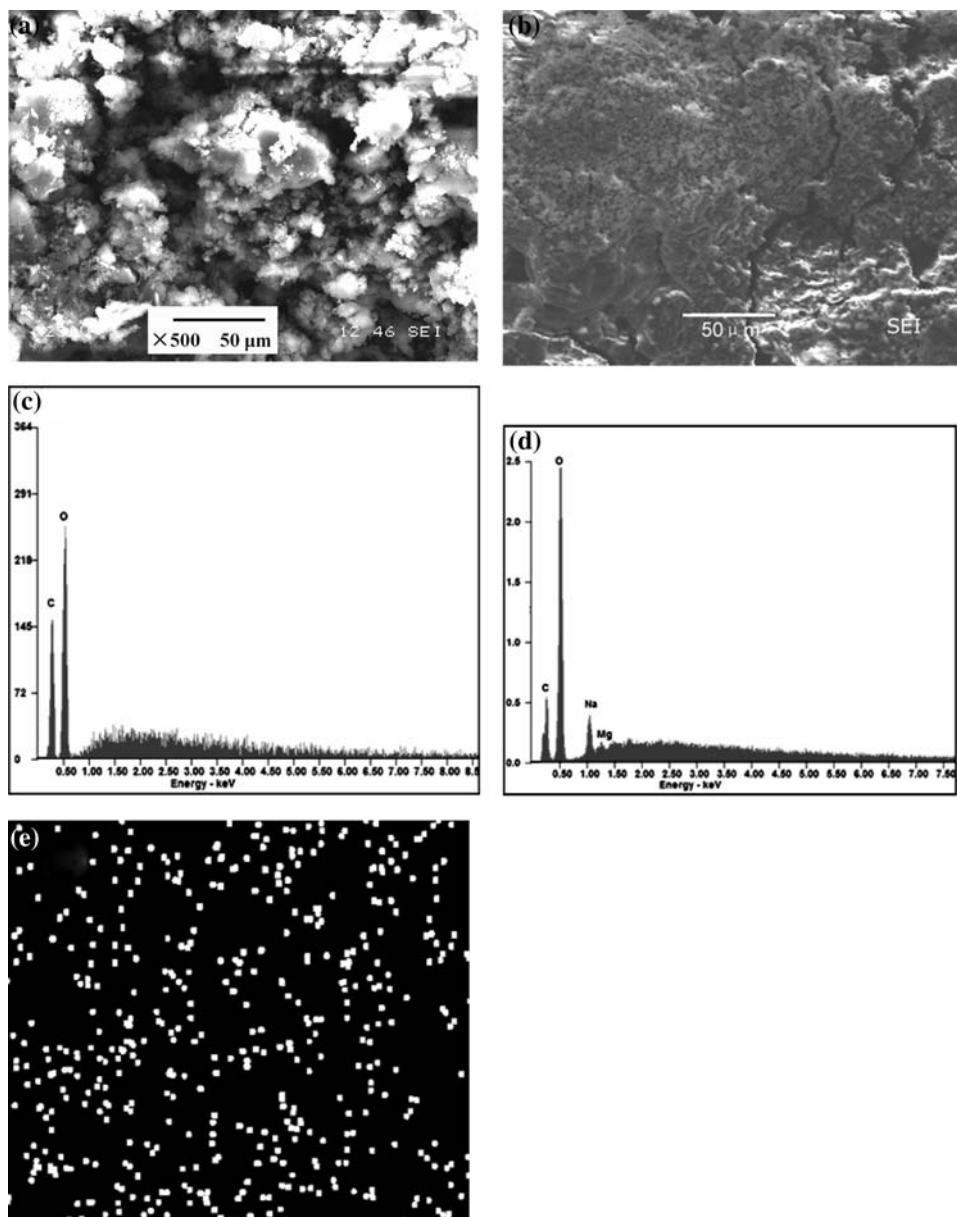
In order to investigate the substance created on the lithium–magnesium anode surface film, the phase composition of the surface film was tested via XRD. It was difficult to detect the existence of Mg on the surface of Li-0.07 wt% Mg due to its low Mg content. Li-5 wt% Mg was selected as the sample of XRD to investigate the effect of adding magnesium to lithium at the anode. In the presence of additives, X-ray diffraction (XRD) patterns of the lithium–magnesium alloy surface in saturated lithium hydroxide electrolyte containing sodium hydroxide after discharge are given in Fig. 10. After discharge the lithium–magnesium alloy surface mainly consisted of a large amount of LiOH, LiOH·H<sub>2</sub>O, and some Mg(OH)<sub>2</sub>.

## 4 Discussions

A porous lithium hydroxide film forms on the lithium metal surface when it discharges in aqueous solutions [2–9]. The behavior of the hydrogen evolution reaction and the



**Fig. 9** Morphology of lithium in saturated lithium hydroxide and Li–1.16 wt% Mg alloy in the saturated lithium hydroxide with sodium hydroxide and additives after discharge at 25 °C. **a** Secondary electron image (SEI) of lithium; **b** secondary electron image (SEI) of Li–1.16 wt% Mg alloy; **c** energy spectrum analysis of the lithium anode surface after discharge; **d** energy spectrum analysis of Li–1.16 wt% Mg anode surface after discharge; **e** distribution of Mg on the surface of Li–1.16 wt% Mg anode. The electrolyte was not circulated



discharge performance are dependent on the property and integrity of the surface film when lithium discharges. Alloying the anode has two functions, namely, altering the surface film and creating a micro-cell. Magnesium is added to the lithium anode.  $\text{Mg}(\text{OH})_2$  is created on the surface film of the lithium–magnesium alloy during its discharge (Fig. 10). On one hand,  $\text{Mg}(\text{OH})_2$  makes the lithium–magnesium surface film more compact and stable (Fig. 9b) after discharge which blocks the direct reaction of the anode with water. As a result, the hydrogen evolution rate of lithium–magnesium is lower than that of the lithium anode (Fig. 4). On the other hand, a micro-cell comprised of lithium and magnesium is created in the alloy, which causes that the micro-cell corrosion current of lithium–magnesium is higher than that of lithium (Table 1).

When magnesium content is lower (0.07 wt% Mg), the micro-cell corrosion current of the lithium–magnesium anode is slightly higher than that of the lithium anode (Table 1). The blockage of direct lithium–water chemical reaction from  $\text{Mg}(\text{OH})_2$  created on the anode surface film plays the primary role. Addition of 0.07 wt% Mg to the lithium anode clearly decreases hydrogen evolution reaction of the lithium anode. The open circuit potential of Li–0.07 wt% Mg is slightly more positive than that of lithium (Table 1), and the anodic polarization current density has small changes. Consequently, addition of 0.07 wt% Mg to the lithium anode has a comparatively small effect on discharge current.

When magnesium content is higher (1.16 wt% Mg), the micro-cell corrosion current of the lithium–magnesium

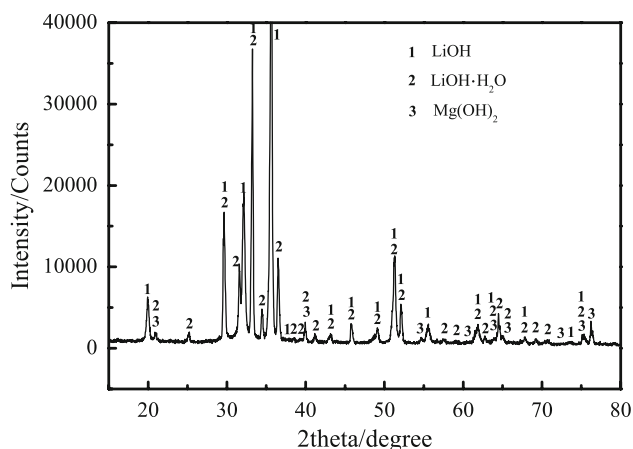


**Fig. 10** Phase composition of Li-5 wt% Mg alloy surface in the saturated lithium hydroxide with sodium hydroxide and additives after discharge at 25 °C. The electrolyte was not circulated

anode is much higher than that of the lithium anode (Table 1). The higher micro-cell corrosion current partly counteracts the hydrogen inhibition effect of  $\text{Mg}(\text{OH})_2$  blockage on the direct lithium–water chemical reaction. Therefore, the hydrogen inhibition effect of Li-1.16 wt% Mg is weaker than that of Li-0.07 wt% Mg (Fig. 4). The open circuit potential of Li-1.16 wt% Mg is much more positive than that of the lithium anode (Table 1). The anodic polarization current density decreases significantly. As a result, the anodic discharge current density decreases with addition of 1.16 wt% Mg to the lithium anode (Fig. 5). Therefore, excessively adding magnesium to the lithium anode is inappropriate in order to decrease hydrogen evolution and maintain high discharge current density at the lithium anode.

## 5 Conclusions

- (1) The surface film on the lithium–magnesium anode after discharge contained  $\text{Mg}(\text{OH})_2$ . The lithium–magnesium surface film is less porous than the lithium surface film.
- (2) Addition of 0.07 wt% Mg to the lithium anode can decrease hydrogen evolution corrosion, enhance discharge current efficiency, and maintain higher discharge current density of the anode.
- (3) Addition of 1.16 wt% Mg to the lithium anode decreased the discharge current. The discharge potential of the Li-1.16 wt% Mg anode is more positive than that of the lithium anode. The effect of micro-cell corrosion created in Li-1.16 wt% Mg alloy anode partly counteracts the hydrogen inhibition effect of  $\text{Mg}(\text{OH})_2$  blockage on the direct lithium–water chemical reaction.

**Acknowledgments** The author gratefully acknowledges the analytical support by State Key Laboratory of Powder Metallurgy, Central South University. The authors also greatly acknowledged the financial support by National Basic Research Program of China (No. 2005CB623704) and Project supported by the Foundation for Innovative Research Groups of the National Natural Science Foundation of China (No. 50721003).

## References

1. Flores JR (1999) Electrochemical studies of lithium/water systems for the development of long life-low power aqueous lithium battery. Master thesis, Pennsylvania State University
2. Littauer EL, Tsai KC (1976) Anodic behavior of lithium in electrolytes. I. Transient passivation. *J Electrochem Soc* 123(6): 771–776
3. Littauer EL, Momyer WR, Tsai KC (1977) Current efficiency in the lithium–water battery. *J Power Sources* 2(2):163–176
4. Littauer EL, Tsai KC (1977) Corrosion of lithium in alkaline solution. *J Electrochem Soc* 124(6):850–855
5. Littauer EL, Tsai KC, Hollandsworth RP (1978) Anodic behavior of lithium in aqueous electrolytes. III. Influence of flow velocity, contact pressure, and concentration. *J Electrochem Soc* 125(6): 845–852
6. Littauer EL, Tsai KC (1976) Anodic behavior of lithium in aqueous electrolytes. II. Mechanical passivation. *J Electrochem Soc* 123(7):964–969
7. Littauer EL, Tsai KC (1980) Anodic behavior of lithium in aqueous electrolytes. IV. Influence of temperature. *J Electrochem Soc* 127(3):521–524
8. Urquidi-Macdonald M, Macdonald DD, Pensado-Rodríguez O, Flores JR (2001) The electrochemical behavior of lithium in alkaline aqueous electrolytes. *Electrochim Acta* 47:833–840
9. Pensado-Rodríguez O (1998) The electrochemistry of lithium in alkaline solutions: a model for the lithium films on the metal surface. Ph.D. Thesis, The Pennsylvania State University
10. Urquidi-Macdonald M, Flores JR, Macdonald DD, Pensado Rodríguez O, Van Voorhis D (1998) Lithium/water system: primary batteries. *Electrochim Acta* 43:3069–3077
11. Tsai KC, Littauer EL (1976) Electrolyte compositions. US Patent 3,976,509
12. Pensado-Rodríguez O, Urquidi-Macdonald M, Macdonald DD (1999) Electrochemical behavior of lithium in alkaline aqueous electrolytes. I. Thermodynamics. *J Electrochem Soc* 146(4): 1318–1325
13. Pensado-Rodríguez O, Flores JR, Urquidi-Macdonald M, Macdonald DD (1999) Electrochemical behavior of lithium in alkaline aqueous electrolytes. II. Point defect model. *J Electrochem Soc* 146(4):1326–1335
14. Urquidi-Macdonald M, Castaneda H, Cannon AM (2002) Lithium fuel cells: I. Lithium/poly(organophosphazene) membrane anodes in KOH and seawater. *Electrochim Acta* 47:2495–2503
15. Zhang Y, Urquidi-Macdonald M (2004) Highly efficient lithium composite anode with hydrophobic molten salt in seawater. *J Power Sources* 129:312–318
16. Zhang Y, Urquidi-Macdonald M (2005) Hydrophobic ionic liquids based on the 1-butyl-3-methylimidazolium cation for lithium/seawater batteries. *J Power Sources* 144:191–196
17. Shuster N (1992) Lithium–water power source for low power long duration undersea application. In: Proceedings of the 35th international power sources symposium, IEEE, p 118
18. Shuster N (1995) US Patent 5,427,873, June 27
19. Urquidi-Macdonald M, Cho JJ (2000) Study of lithium polymer interface to enhance efficiency and safety in lithium/water batteries,

- In: Proceedings of IMECE: International mechanical engineering congress and exposition, Paper 2633 ASTM, November 5–10, Walt Disney World Dolphin, Orlando, FL 366(1):11–18
20. Shin K (1982) Silver-oxide lithium aqueous-solution battery, JP57017565,311-312
  21. Urbach HB, Icenhower DE, Cervi MC, Bowen RJ (1976) Electrochemical cell using lithium–aluminum alloy anode and aqueous electrolyte. US Patent, 3980498, September 14
  22. Liu K (1987) Inorganic chemistry, 1st edn. Chengdu University of Science and Technology Press, Chengdu, p 291
  23. Massalski TB, Murray JL, Bennett LH, Baker H (1986) Binary alloy phase diagrams, Vol. 2, American Society for Metals, Metals Park, OH, pp 1487
  24. Fu C (2005) Study of Li–H<sub>2</sub>O battery and inhibitors in alkaline solution. Master thesis. Huazhong University of Science & Technology, Wuhan, China